Journal of Materials Chemistry C

PAPER

Cite this: DOI: 10.1039/c3tc32259a

Correlation between preparation conditions and the photoluminescence properties of Sn^{2+} centers in $ZnO–P_2O_5$ glasses†

Hirokazu Masai,*[a] Toshiro Tanimoto,[a] Shun Okumura,[a] Kentaro Teramura,[b] Syuji Matsumoto,[c] Takayuki Yanagida,[d] Yomei Tokuda[a] and Toshinobu Yoko[a]

Received 15th November 2013
Accepted 3rd January 2014

DOI: 10.1039/c3tc32259a

www.rsc.org/MaterialsC

Photoluminescence (PL) and coordination states of Sn^{2+} centers in $1SnO–68ZnO–31P_2O_5$ (SZP31) glass prepared under different conditions are examined. When prepared in air, the local coordination state of Sn^{2+} centers depends on the starting material. In contrast, the PL properties of Sn^{2+} centers of the glass prepared under inert atmosphere conditions are independent of the starting material because of elimination of the oxidation reaction. ^{119m}Sn Mössbauer and X-ray absorption fine structure analyses indicate that most of the Sn^{2+} centers in the SZP31 glass prepared in an inert atmosphere exist at a SnO-like coordination state, possessing a coordination number greater than 2. It is assumed that the more highly coordinated Sn^{2+} is the origin of high PL intensity with high quantum efficiency.

1. Introduction

Phosphors are solid luminescent materials that have several applications in our daily lives. From the viewpoint of the luminescence process, phosphors can be classified into two types: activator (emission center)-containing materials and self-activated materials.[1] Most phosphors belong to the former group, and the rare earth (RE) cation is a typical emission center needed for a phosphor to exhibit a sharp emission band.[1] Further, RE-free phosphors will continue to attract attention not only because they are composed of ubiquitous elements but also because of their characteristic emission properties. In contrast to conventional RE cations possessing a narrow emission band due to the f–f transition,[1–6] other metal oxides can exhibit tunable emission properties that are affected by the coordination field.[1,7–15] Among non-RE emission centers, the ns^2-type emission center is one of the most promising ones exhibiting high emission intensity due to the parity-allowed excitation ($^1S_0 \rightarrow {}^1P_1$). In addition, the emission can be tailored by tuning the local coordination state because the centers ($n \geqq 4$) possess an electron in the outermost shell in both the ground state (ns^2) and the excited state (ns^1np^1). Moreover, this emission center generally takes the metastable valence of each element, which is the reason why the number of crystals containing these species is not very large. Therefore, this type of emission center can be considered to be more suitable for amorphous materials whose site distribution is much wider than that of crystals.

Recently, our group has demonstrated a high photoluminescence (PL) efficiency of RE-free $SnO–ZnO–P_2O_5$ (SZP) glass.[16,17] The emission is due to the Sn^{2+} center belonging to the ns^2-type emission centers. Compared with other ns^2-type centers such as Sb^{3+}, Tl^+, and Pb^{2+}, the Sn^{2+} center has an advantage from the viewpoint of ubiquitous and harmless elements. It is notable that the transparent glass containing no RE cation shows a high UV-excited emission comparable to those of crystal phosphors such as $MgWO_4$. Furthermore, the reported PL efficiency was the largest ever reported for a glass material without a RE cation. In addition, the UV-excited white light emission properties of MnO-codoped SZP glasses were also demonstrated.[18–20] The white light emission, consisting of broad bands, can be tailored by the addition of a Mn^{2+} emission center instead of a RE emission center. Because the Sn^{2+}-containing zinc phosphate glasses also exhibit scintillation behavior,[21,22] the dependence of the emission behavior of Sn^{2+} on the excitation light source is also an attractive possibility. More recently, we have examined the correlation between the emission properties and the amount of SnO in the SZP glass.[23,24] It was found that two PL excitation (PLE) bands exist in the SZP glasses and that the PLE band at lower peak energy, which is the origin of the optical absorption edge, strongly depends on the SnO concentration.

However, neither the correlation between the actual concentration of Sn^{2+} centers and emission properties nor the local coordination states of Sn^{2+} centers has been fully clarified

[a]Institute for Chemical Research, Kyoto University, Gokasho, Uji, Kyoto 611-0011, Japan. E-mail: masai_h@noncry.kuicr.kyoto-u.ac.jp
[b]Department of Molecular Engineering, Kyoto University, Kyotodaigaku Katsura, Nishikyo-ku, Kyoto 615-8510, Japan
[c]Research Center, Asahi Glass Co., Ltd. 1150, Hazawa-cho, Kanagawa-ku, Yokohama 211-8755, Japan
[d]Kyushu Institute of Technology, 2-4, Hibikino, Wakamatsu-ku, Kitakyushu 808-0196, Japan

† Electronic supplementary information (ESI) available. See DOI: 10.1039/c3tc32259a

because the SZP glasses in previous studies were prepared under ambient air conditions. Because it is often reported that Sn^{2+} of SZP glass is oxidized to Sn^{4+} over 800 °C,[25] it is necessary to control the oxidation state of Sn in order to discuss the local coordination field in the glass. Using Mössbauer spectroscopy, it was estimated that the oxidation states of Sn in 2.5SnO–57.5ZnO–40P_2O_5 glass corresponded to Sn^{2+} (89%) and Sn^{4+} (11%).[16,17] Several papers concerning emission of Sn^{2+} also suggest oxidation of Sn^{2+} during the preparation or melting processes.[26–28] Although it is expected that oxidation of Sn^{2+} to Sn^{4+} affects the emission properties, the effect of Sn^{4+} on SZP glass emission properties has not been clarified yet.[16–22] Therefore, it is important to examine the correlation between preparation conditions and physical parameters of SZP glass for practical applications.

One of the aims of the present study is to examine the relationship between emission properties (PL intensity or PLE peak) of SZP glass and the preparation conditions. Different starting chemicals or different atmosphere conditions may change the redox state of the cation. To examine the physical properties of SZP glass using $Zn_2P_2O_7$ as a starting material (SM), the chemical composition for the study was selected as 1SnO–68ZnO–31P_2O_5 (in molar ratio) because SZP glass possessing a stoichiometric chemical composition of $Zn_2P_2O_7$ (1SnO–66ZnO–33P_2O_5) was easily crystallized during the melt-quenching. Herein, this glass system is denoted as SZP31.

Another aim of this study is to examine local coordination states of Sn^{2+} emission centers based on the two PLE peaks. Although we have hypothesized that the two excitation bands of the SZP glass originate in different coordination states of Sn^{2+} emission center, our hypothesis is not very strong because Sn^{2+} and Sn^{4+} species coexist in the SZP glass prepared in air. In this study, we have examined the local coordination states of Sn^{2+} centers of SZP31 glasses containing the Sn^{2+} species, using X-ray absorption fine structure (XAFS) analysis. Local coordination states of Sn^{2+} centers in SZP glass are discussed on the basis of the results of Mössbauer spectroscopy and XAFS analyses.

2. Experimental section

Sample preparation in air

The present 1SnO–68ZnO–31P_2O_5 (SZP31) glass was prepared according to a conventional melt-quenching method by employing a platinum crucible.[29] Starting P_2O_5-component chemicals were $Zn_2P_2O_7$ (99.9%, Kojundo Chemical Laboratory Co., Ltd.), P_2O_5 (99.999%, Kojundo Chemical Laboratory Co., Ltd.), and $(NH_4)_2HPO_4$ (99.0%, Nacalai Tesque Co., Ltd.). In the case of $(NH_4)_2HPO_4$, the mixture of ZnO and $(NH_4)_2HPO_4$ was initially calcined at 800 °C for 3 h using a Pt crucible in an ambient atmosphere. After treatment, the calcined matrix was mixed with SnO and melted in an electric furnace at 1100 °C for 30 min in an ambient atmosphere. For the addition of the reducing agent (C), SnO and C were simultaneously added into the calcined mixture before melting. The glass melt was quenched on a stainless plate at 200 °C and then annealed at T_g, which was measured by differential thermal analysis (DTA), for 1 h. On the other hand, when $Zn_2P_2O_7$ or P_2O_5 was used instead of $(NH_4)_2HPO_4$, the mixture of SnO, ZnO, and a phosphorus source were melted under the same conditions without the calcination process. Quenching and annealing processes followed as mentioned above.

Sample preparation in an inert atmosphere

In the case of preparation in the inert atmosphere (Ar), a batch consisting of ZnO and a phosphorus source was first calcined in air and then mixed with SnO at r.t. The mixture was set in the atmosphere-controlled electric furnace at r.t. It took 2 h to heat up from r.t. to 1100 °C, and the temperature was fixed at 1100 °C for 30 min. After melting, glass melt was also quenched on a stainless plate at 200 °C and then annealed at T_g for 1 h.

Characterization

T_g was determined by a DTA system operating at a heating rate of 10 °C min^{-1} using a TG8120 (Rigaku, Japan). The PL and PLE spectra were recorded at room temperature (r.t.) using a Hitachi 850 fluorescence spectrophotometer. Band pass filters for the PL measurement were used for the excitation (5 nm) and the emission (3 nm). The absorption spectra at r.t. were recorded using a U3500 UV-vis-NIR spectrometer (Hitachi High-Tech. Japan). The absolute quantum efficiency and color coordination position of emission of the glass were measured using an integrating sphere C9920-02 (Hamamatsu Photonics, Japan) at r.t. The emission decay at r.t. was measured using a Quantaurus-Tau (Hamamatsu Photonics, Japan) with a 280 nm LED. The absolute quantum efficiency of the glass was measured using a Quantaurus-QY (Hamamatsu Photonics, Japan). ^{119m}Sn Mössbauer spectra at r.t. were obtained in transmission geometry.

The Sn K-edge (29.3 keV) XAFS spectra were recorded at BL01B1 of SPring-8 (Hyogo, Japan). The storage ring energy was operated at 8 GeV with a typical current of 100 mA. The measurements were carried out using a Si (311) double crystal monochromator in the transmission mode (Quick Scan method) at r.t. XAFS data of Sn-foil, SnO, and SnO_2 were also collected using the same conditions. Using REX2000 software (Rigaku), fitting was performed by the nonlinear least-squares method. Values for the backscattering factor and the phase shift were taken from McKale's table.[30]

3. Results and discussion

3.1. SZP31 glasses melted in air

The SZP31 glasses melted in air were colorless and transparent. Table 1 lists glass transition temperatures, T_g, of these glasses. T_g of the glasses melted in air was about 449 °C, and no

Table 1 T_g of the SZP31 glasses prepared in air using different starting materials

	Starting chemicals		
	P_2O_5	$(NH_4)_2HPO_4$	$Zn_2P_2O_7$
T_g/°C	447	449	452

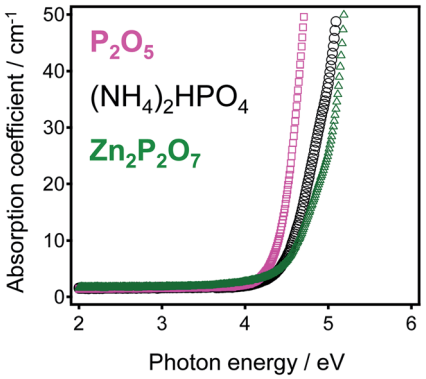

Fig. 1 Optical absorption spectra of three SZP31 glasses prepared in air using different starting materials.

significant difference was observed in T_g based on the different starting materials. Fig. 1 shows the optical absorption spectra of three SZP31 glasses whose phosphorous SMs are $Zn_2P_2O_7$, $(NH_4)_2HPO_4$, and P_2O_5. The order of observed red-shift of the absorption edge in the SZP31 glasses was as follows in terms of the SM: $Zn_2P_2O_7$ < $(NH_4)_2HPO_4$ < P_2O_5 as a SM. It was found that the absorption edge of the SZP glass correlated with the local coordination state of the Sn^{2+} emission center.[23,24] This relationship was also observed in other oxide glass phosphors containing ns^2-type emission centers.[31,32] Therefore, it was expected that the observed shift of the absorption edge suggested that the coordination state of the Sn^{2+} center changes depending on the SM. PL-PLE spectra of these glasses are shown in Fig. 2. The emission intensity of PL-PLE spectra of the SZP glass prepared from P_2O_5 was much higher than those of other glasses. On the other hand, the Stokes shift, the energy difference between PLE and PL peaks, also decreased in the following order of SM: $Zn_2P_2O_7$ > $(NH_4)_2HPO_4$ > P_2O_5, which corresponds to change of the optical absorption edge as shown in Fig. 1. Such a red-shift of the optical absorption edge and PLE peak has already been observed in a previous report in which the optical absorption edge was red-shifted with increasing amount of SnO in xSnO–60ZnO–40P_2O_5 glasses, and the resulting Stokes shift became smaller.[23,24] Fig. 3 shows emission decay curves of the SZP31 glasses. The decays consist of two parts: a faster decay with a lifetime on the order of a few nanoseconds and a slower decay with a lifetime of microseconds. Considering the emission intensities of these glasses shown in Fig. 2, we attributed the decay with a lifetime on the order of a few nanoseconds, which depended on the starting material, to $S_1 \rightarrow S_0$ non-radiative transitions; further, we considered that the decay with the order of lifetimes of microseconds and $\tau_{1/e} \sim 3.7$ μs, and that is independent of the SM, was due to $T_1 \rightarrow S_0$ radiative transitions.[1,21–28] Thus, it is expected that the actual number of Sn^{2+} centers in the SZP31 glass prepared from P_2O_5 in air is higher than that in other glasses, although the nominal chemical composition is fixed, and that the less-oxidized state is generated by using P_2O_5 as a SM. In other words, the Sn^{2+} content of glass melt in air is affected by the SM, and some of the Sn^{2+} species is oxidized into Sn^{4+}. Although no clear evidence was obtained, we speculate that P_2O_5, which has the lowest melt temperature, reacts with SnO to form a surrounding layer to prevent oxidation during the initial melt process. However, no significant difference was observed in T_g among SZP31 glasses prepared from different SMs. Because the three glasses showed similar T_g values, it was assumed that generated Sn^{4+} facilitates the increase in the glass network T_g, which is not sensitive to the concentration of Sn^{4+}. Although SZP31 glass prepared with P_2O_5 possesses higher emission intensity, handling of this chemical is difficult because of the strong hygroscopicity. Thus, preparation of SZP31 glass using $(NH_4)_2HPO_4$ in an inert atmosphere was examined instead.

3.2. SZP31 glasses melted in an inert atmosphere

As discussed above, oxide glass prepared by the melt-quenching method is usually affected by the preparation process even though the nominal chemical composition remains fixed. In particular, valence control of the cation is important for glassy materials.[33–35] In order to examine the relationship between preparation conditions and optical properties, SZP31 glasses were prepared using $(NH_4)_2HPO_4$ both in air and in an inert atmosphere. Fig. 4 shows optical absorption spectra and PLE spectra of SZP31 glasses melted in air and in Ar. The PL peak

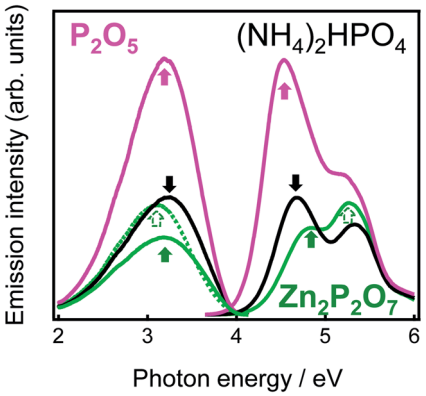

Fig. 2 PL-PLE spectra of three SZP31 glasses prepared in air from $Zn_2P_2O_7$, $(NH_4)_2HPO_4$, and P_2O_5 starting materials.

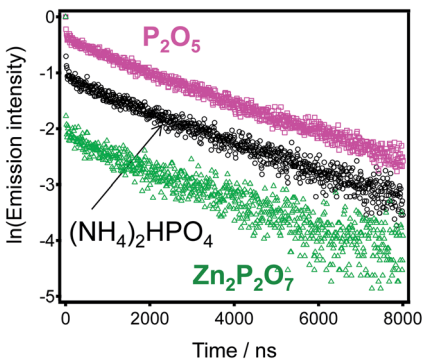

Fig. 3 Emission decay curves of the SZP31 glasses prepared by use of three different starting chemicals (excitation: 280 nm and emission: 400 nm).

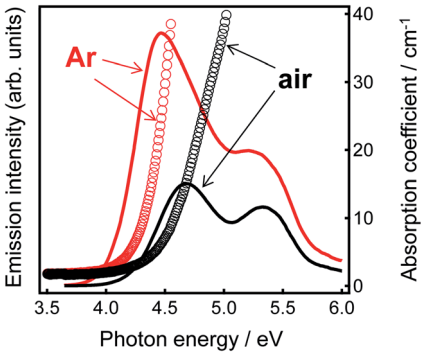

Fig. 4 PLE spectra and absorption spectra of the SZP31 glasses prepared in air and in an Ar atmosphere.

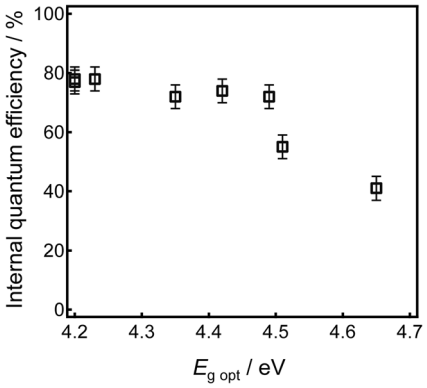

Fig. 5 Relationship between $E_{g,opt}$ and internal quantum efficiency of the SZP31 glasses prepared in air and in Ar.

intensity of SZP31 glass prepared in Ar is more than twice that of the glass prepared in air. In particular, the intensity of the lower excitation band is enhanced by the inert preparation. Both the optical absorption edge and the PLE peak of the glass melted in Ar red-shift compared to those of the glass melted in air. Considering the red-shift of PLE peaks of the SZP glasses melted in Ar, it was concluded that the actual concentration of Sn^{2+} centers of the SZP31 glass melted in Ar was much higher than that of the one melted in air.

Further, we prepared SZP31 glass with the addition of the reducing agent C in an Ar atmosphere in order to examine the possibility that Sn^{4+} was present in the starting material. PL-PLE spectra of these glasses with and without a reducing agent indicated that Sn^{4+} can be ignored as an impurity in the starting batch (see ESI Fig. 1†). T_g values of these SZP31 glasses are shown in Table 2. T_g values of the SZP31 glasses melted in the Ar atmosphere were about 10 °C lower than for the glass melted in air. It was found that neither the addition of carbon nor a change in the starting materials affected T_g. It was, therefore, concluded that the starting material did not affect the oxidation of Sn^{2+} during the melting process and that Sn^{2+} was not oxidized by melting in an inert atmosphere. It is expected that almost 100% of Sn is in the Sn^{2+} state in the SZP31 glass melted in Ar, and the ratio is independent of the starting material. The decrease in T_g by melting in the Ar atmosphere suggests that only 1 mol% of Sn species was sufficient to affect the macroscopic thermal properties, *i.e.*, network formation, of glass. It was reported that there is a correlation between optical energy gap, $E_{g,opt}$, and PLE peak energy.[23,24] Fig. 5 shows the relationship between $E_{g,opt}$ and the internal quantum efficiency of the SZP31 glasses prepared in air and in Ar. There is a correlation between quantum efficiency and $E_{g,opt}$ values, indicating that the less $E_{g,opt}$ changes, the higher quantum efficiency intensity becomes. The relationship also suggests that no apparent concentration quenching is observed in this Sn^{2+} fraction. The SZP31 glass prepared in an Ar atmosphere center exhibits a high internal quantum efficiency of 78% (by excitation at 280 nm) and an $E_{g,opt}$ of 4.2 eV. The obtained relationship suggests that the degree of oxidation reaction from Sn^{2+} to Sn^{4+} may be roughly estimated from this $E_{g,opt}$ value.

Table 2 T_g of the SZP31 glasses prepared in Ar using different starting materials

	Starting chemicals			
	P_2O_5	$(NH_4)_2HPO_4$		$Zn_2P_2O_7$
T_g/°C	440	438	440 (+0.1 mol% C)	441

3.3. Examination of local coordination states of Sn^{2+} centers

As shown in Fig. 4, it was found that the emission properties of Sn^{2+} centers in SZP31 glass strongly depended on the preparation atmosphere. Comparing these two samples, we noticed that the peak intensity of the lower-energy band is much higher than that of the higher-energy band of SZP glass melted in Ar. Because it was reported that the Sn^{2+} center possessing C_{2v} symmetry in SiO_2 glass exhibits the S_1 excitation band at 4.9 eV,[36] we determined that the higher-energy band is due to 2-coordinated Sn^{2+} whereas the lower band is due to the Sn^{2+} center possessing a high coordination number.[23,24] In order to prove this hypothesis, we examined the relationship between the emission properties and the local structure of Sn species in the glasses melted in different atmospheres.

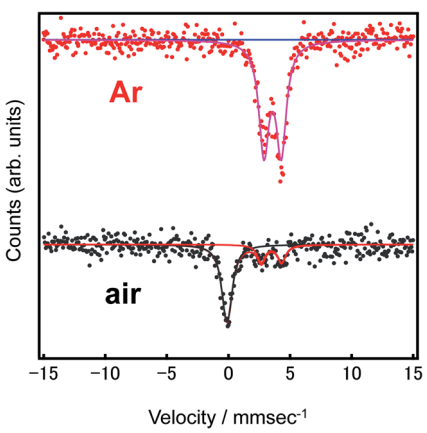

Fig. 6 ^{119m}Sn Mössbauer spectra of SZP31 glasses prepared in air and in an Ar atmosphere.

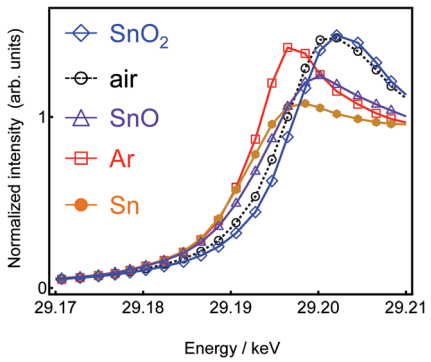

Fig. 7 Sn K-edge XANES spectra of the SZP31 glasses prepared in air and in Ar along with those of Sn, SnO, and SnO_2 for reference.

Fig. 6 shows the ^{119m}Sn Mössbauer spectra of the glasses melted under different atmospheric conditions. The peak at 0 mm s^{-1} corresponds to the Sn^{4+} species, whereas the peak at 3–4 mm s^{-1} corresponds to the Sn^{2+} species.[37–41] The figure shows that most of the Sn in the glass melted in air exists as Sn^{4+}, whereas Sn^{4+} was not observed in the glass melted in an Ar atmosphere. After peak deconvolution,[42] the amounts of Sn^{2+} in SZP31 glass melted in air and in Ar were calculated to be 14 ± 2% and ~100%, respectively. This valence change of Sn^{2+} corresponds to our expectation as mentioned previously. The valence state of the Sn species was also estimated from Sn K-edge XANES spectra, as shown in Fig. 7. Because a higher absorption edge indicated a higher oxidation state of the cation, we took absorption edge energy, E_0, to be the energy at the zero-crossing of the 2nd derivative. The Sn K-edge energy of SZP31 glass melted in Ar was similar to that of SnO, and lower than that of glass melted in air, indicating that the SZP31 glass melted in Ar contains a higher number of Sn^{2+} centers. From each E_0 value, $|\Delta(E_0(\text{Sn-foil}) - E_0(\text{glass, Ar}))|$ and $|\Delta(E_0(\text{SnO}) - E_0(\text{glass, Ar}))|$ were calculated to be less than 1.7 eV. Considering the resolution of the measurement ($\Delta E/E \sim 6 \times 10^{-5}$), we assumed that this difference (less than 1.75 eV) was insignificant. Thus, Sn K-edge XAFS also supported the hypothesis that the percentage of Sn^{2+} to total Sn in SZP31 glass melted in Ar is almost 100%. From Mössbauer and Sn K-edge XANES spectra results, we assume that the actual number of Sn^{2+} centers governs the PLE spectra shape, *i.e.*, PLE spectra are independent of the amount of Sn^{4+}.

Fig. 8a shows EXAFS spectra $k^3\chi(k)$ of SZP31 glasses prepared by melting in different atmospheres along with spectra of SnO and SnO_2. k is the wavenumber of the photoelectron. Comparing the spectra of the two SZP31 glasses, we noticed the following: (1) the amplitude of SZP31 glass prepared in Ar was smaller than those of other samples. (2) The oscillation of SZP31 glass prepared in Ar was similar to that of SnO, whereas that of SZP31 glass prepared in air was similar to SnO_2. Fig. 8b shows the Fourier-transform (FT) of EXAFS spectra of two SZP31 glasses along with SnO and SnO_2. Although the peak of the second coordination sphere can be observed in the spectrum of standard materials, only the peak of the first coordination sphere of Sn was identified in the SZP31 glasses. Therefore, the coordination number and the coordination distance of Sn in the SZP31 glasses

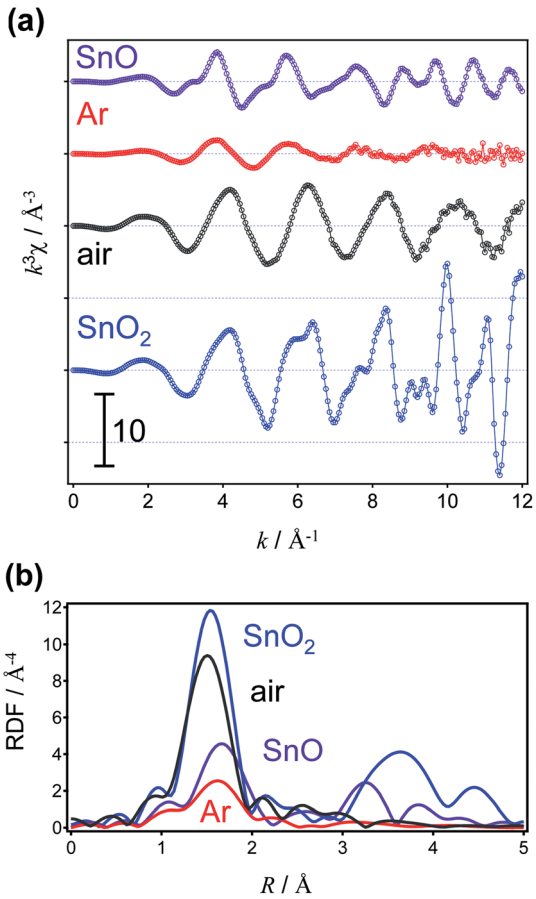

Fig. 8 (a) EXAFS spectra $k^3\chi(k)$ of SZP31 glasses prepared by melting in different atmospheres along with SnO and SnO_2 for reference. (b) FT of EXAFS spectra of the two SZP31 glasses along with SnO and SnO_2.

were estimated by fitting of the first coordination sphere in the EXAFS spectra. The fitting results of the SZP31 glasses are shown in Table 3 along with those of SnO and SnO_2. The SnO and SnO_2 coordination numbers and Sn–O coordination lengths both correspond to those in reference data.[43,44] From ^{119m}Sn Mössbauer and Sn K-edge XANES spectra, we determined that only Sn^{2+} existed in the SZP31 glass melted in an Ar atmosphere. Therefore, the calculated parameter shows average coordination states of Sn^{2+} species in the SZP31 glass melted in an Ar atmosphere. Because the coordination number and coordination length values are similar to those of the SnO crystal, it is expected that the Sn^{2+} center in the SZP31 glass takes a similar structure to

Table 3 First-shell Sn–O fitting results for the SZP31 glasses. The reported data of SnO[43] and SnO_2 (ref. 44) are also shown for comparison

	SZP31 glass		Reference	
	Ar	Air	SnO	SnO_2
Coordination number	4.2	5.1	4.0 (4.0)[43]	5.8 (6.0)[44]
Distance of Sn–O/Å	2.16	2.02	2.21 (2.22)[43]	2.05 (2.06)[44]

that of the SnO crystal possessing a 4-coodinated state. On the other hand, the SZP31 glass melted in air, containing both Sn^{2+} and Sn^{4+}, exhibits structural parameters close to those of SnO_2, indicating that Sn^{4+}, the major tin species in this glass, takes a similar structure to the SnO_2 crystal.

Here, we have discussed the coordination state of the Sn^{2+} center in the SZP glasses. In the PLE spectra of SZP glass containing different amounts of SnO, the peak area of the higher excitation band around 5 eV was saturated after 0.1 mol% addition of SnO whereas that of the lower-energy band increased with increasing amount of SnO.[23,24] Therefore, we assume that only a small number of two-coordinated Sn^{2+} centers can exist in oxidized glass. Because the concentration of Sn^{2+} in the tested SZP31 glass was 1 mol%, which is much higher than that used in previous reports on 2-coordinated Sn^{2+} centers, XAFS analysis of the SZP glass prepared under inert conditions showed the average coordination data for the Sn^{2+} species: 2-coordinated and higher-coordinated states. Thus, it is expected that the 2-coordinated Sn^{2+} center only exists in very small numbers compared to the Sn^{2+} possessing a higher coordination number, and that the higher-coordinated Sn^{2+} center, which were determined as the origin of the low-energy band, is the dominant structure in the SZP31 glass. Although the precise structure has not yet been clarified, the coordination state of higher-coordinated Sn^{2+} species in the glass appears to be close to that of the SnO crystal in which Sn takes a 4-coordination state.

It is often reported that phosphate glasses show poor chemical durability that limits the application field. However, not all phosphate glasses show low chemical durability.[45–48] We have recently reported phosphate glass exhibiting high water durability because of the lack of phosphate chain units.[48] On the other hand, we have also demonstrated that the PL properties of the Sn^{2+} emission center were affected not by the average (macroscopic) basicity of the phosphate glass, but by the local coordination field.[24] These findings suggest that phosphate-based glass can be a practical host for emission centers by tailoring the random network in the future.

4. Conclusion

We have examined the correlation between the emission spectra of Sn^{2+} centers and the local coordination states in the SZP31 glasses. It was found that the oxidation of Sn^{2+} during preparation was effectively prevented by melting in an inert atmosphere. Both absorption and PLE spectra depended on the actual number of Sn^{2+} centers in the glass. In the SZP31 glass, the coordination state of Sn^{2+} is similar to that of Sn^{2+} in SnO crystals, whereas the coordination state of Sn^{4+} in the glass is similar to that of Sn^{4+} in SnO_2 crystals. Because most Sn^{2+} centers take on a coordination state higher than 2, it was determined that the coordination state was the origin of the PLE band at lower photon energy that accompanies high quantum efficiency.

Acknowledgements

This work was partially supported by the Asahi Glass Foundation, the Kazuchika Okura Memorial Foundation, the Research Institute for Production Development, and the Collaborative Research Program of Institute for Chemical Research, Kyoto University (grant # 2013-62).

References

1 S. Tanimizu, in *Phosphor handbook 2nd edition*, ed. W. M. Yen, S. Shionoya and H. Yamamoto, CRC Press, Boca Raton, U.S.A, 2007.
2 D. L. Dexter, *J. Chem. Phys.*, 1953, **21**, 836.
3 J. E. Geusic, H. M. Marcos and L. G. Vanuitert, *Appl. Phys. Lett.*, 1964, **4**, 182.
4 T. Matsuzawa, Y. Aoki, N. Takeuchi and Y. Maruyama, *J. Electrochem. Soc.*, 1996, **143**, 2670.
5 H. A. Hoppe, H. Lutz, P. Morys, W. Schnick and A. Seilmeier, *J. Phys. Chem. Solids*, 2000, **61**, 2001.
6 C. R. Ronda, *J. Lumin.*, 1997, **72**, 49.
7 A. Wachtel, *J. Electrochem. Soc.*, 1966, **113**, 128.
8 Y. Toyozawa and M. Inoue, *J. Phys. Soc. Jpn.*, 1966, **21**, 1663.
9 K. O. Choi, S. W. Lee, H. K. Bae, S. H. Jung, C. K. Chang and J. G. Kang, *J. Chem. Phys.*, 1991, **94**, 6420.
10 K. H. Butler and C. W. Jerome, *J. Electrochem. Soc.*, 1950, **97**, 265.
11 T. S. Davis, E. R. Kreidler, J. A. Parodi and T. F. Soules, *J. Lumin.*, 1971, **4**, 48.
12 T. H. Maiman, *Nature*, 1960, **187**, 493.
13 G. Kemeny and C. H. Haake, *J. Chem. Phys.*, 1960, **33**, 783.
14 C. Barthou, J. Benoit, P. Benalloul and A. Morell, *J. Electrochem. Soc.*, 1994, **141**, 524.
15 M. Liu, A. H. Kital and P. Mascher, *J. Lumin.*, 1992, **54**, 35.
16 H. Masai, Y. Takahashi, T. Fujiwara, S. Matsumoto and T. Yoko, *Appl. Phys. Express*, 2010, **3**, 082102.
17 H. Masai, *J. Ceram. Soc. Jpn.*, 2013, **121**, 150.
18 H. Masai, T. Fujiwara, S. Matsumoto, Y. Takahashi, K. Iwasaki, Y. Tokuda and T. Yoko, *Opt. Lett.*, 2011, **36**, 2868.
19 H. Masai, T. Fujiwara, S. Matsumoto, Y. Takahashi, K. Iwasaki, Y. Tokuda and T. Yoko, *J. Ceram. Soc. Jpn.*, 2011, **119**, 726.
20 H. Masai, T. Fujiwara, S. Matsumoto, Y. Tokuda and T. Yoko, *J. Non-Cryst. Solids*, 2014, **383**, 184.
21 H. Masai, T. Yanagida, Y. Fujimoto, M. Koshimizu and T. Yoko, *Appl. Phys. Lett.*, 2012, **101**, 191906.
22 H. Masai, Y. Hino, T. Yanagida, Y. Fujimoto, K. Fukuda and T. Yoko, *J. Appl. Phys.*, 2013, **114**, 083502.
23 H. Masai, T. Tanimoto, T. Fujiwara, S. Matsumoto, Y. Tokuda and T. Yoko, *Opt. Express*, 2012, **20**, 27319.
24 H. Masai, T. Tanimoto, T. Fujiwara, S. Matsumoto, Y. Tokuda and T. Yoko, *Chem. Lett.*, 2013, **42**, 132.
25 D. R. Lide, *CRC Handbook of Chemistry and Physics*, CRC Press, Boca Raton, FL, USA, 83rd edn, 2002.
26 J. A. Jimenez, S. Lysenko, H. Liu, H. E. Fachini, O. Resto and C. R. Cabrera, *J. Lumin.*, 2009, **129**, 1546.
27 H. Segawa, S. Inoue and K. Nomura, *J. Non-Cryst. Solids*, 2012, **358**, 1333.
28 T. Hayakawa, T. Enomoto and M. Nogami, *Jpn. J. Appl. Phys.*, 2006, **45**, 5078.

29 H. Masai, T. Tanimoto, T. Fujiwara, S. Matsumoto, Y. Takahashi, Y. Tokuda and T. Yoko, *J. Non-Cryst. Solids*, 2012, **358**, 265.

30 A. G. McKale, B. W. Veal, A. P. Paulikas, S. K. Chan and G. S. Knapp, *J. Am. Chem. Soc.*, 1988, **110**, 3763.

31 H. Masai, S. Matsumoto, T. Fujiwara, Y. Tokuda and T. Yoko, *J. Am. Ceram. Soc.*, 2012, **95**, 862.

32 H. Masai, Y. Yamada, S. Okumura, Y. Kanemitsu and T. Yoko, *Opt. Lett.*, 2013, **38**, 3780.

33 H. Masai, K. Hamaguchi, K. Iwasaki, Y. Takahashi, R. Ihara and T. Fujiwara, *Mater. Res. Bull.*, 2012, **47**, 4065.

34 H. Masai, Y. Suzuki, Y. Takahashi, H. Mori, T. Fujiwara and T. Komastu, *J. Ceram. Soc. Jpn.*, 2009, **117**, 671.

35 H. Masai, Y. Yamada, Y. Suzuki, K. Teramura, Y. Kanemitsu and T. Yoko, *Sci. Rep.*, 2013, **3**, 3541.

36 L. Skuja, *J. Non-Cryst. Solids*, 1992, **149**, 77.

37 I. A. Courtney, R. A. Dunlap and J. R. Dahn, *Electrochim. Acta*, 1999, **45**, 51.

38 K. F. E. Williams, C. E. Johnson, J. Greengrass, B. P. Tilley, D. Gelder and J. A. Johnson, *J. Non-Cryst. Solids*, 1997, **211**, 164.

39 P. D. Townsend, N. Can, P. J. Chandler, B. W. Farmery, R. Lopez-Heredero, A. Peto, L. Salvin, D. Underdown and B. Yang, *J. Non-Cryst. Solids*, 1998, **223**, 73.

40 E. Bekaert, L. Montagne, L. Delevoye, G. Palavit and A. Wattiaux, *J. Non-Cryst. Solids*, 2004, **345**, 70.

41 J. P. Bocquet, Y. Y. Chu, O. C. Kistner, M. L. Perlman and G. T. Emery, *Phys. Rev. Lett.*, 1966, **17**, 809.

42 D. Benner, C. Rüssel, M. Menzel and K. D. Becker, *J. Non-Cryst. Solids*, 2004, **337**, 232.

43 F. Izumi, *J. Solid State Chem.*, 1981, **38**, 381.

44 A. A. Bolzan, *Acta Crystallogr., Sect. B: Struct. Sci.*, 1997, **53**, 373.

45 J. Cha, T. Kubo, H. Takebe and M. Kuwabara, *J. Ceram. Soc. Jpn.*, 2008, **116**, 915.

46 Z. Teixeira, O. L. Alves and I. O. Mazali, *J. Am. Ceram. Soc.*, 2007, **90**, 256.

47 T. Harada, H. In, H. Takebe and K. Morinaga, *J. Am. Ceram. Soc.*, 2004, **87**, 408.

48 H. Masai, R. Shirai, Y. Takahashi, T. Fujiwara, Y. Tokuda and T. Yoko, *Chem. Lett.*, 2013, **42**, 1305.